PII: S0032-3861(98)00127-X

Polymer Vol. 39 No. 24 pp. 6145–6151, 1998
0032-3861/98/$ – see front matter

Layer structures 11. Cholesteric polyesters derived from isosorbide, 2,5-bis(dodecyloxy)terephthalic acid and 4,4′-dihydroxybiphenyl

Hans R. Kricheldorf* and Dirk F. Wulff
Institut für Technische und Makromolekulare Chemie der Universität, Bundesstr. 45, D-20146 Hamburg, Germany
(Revised 23 December 1997)

One non chiral homopolyester and five chiral copolyesters were prepared by polycondensations of 2,5-bis(dodecyloxy)terephthaloylchloride and 4,4′-dihydroxybiphenyl or mixtures of this diphenol and isosorbide. The resulting polyesters were characterized by viscosity measurements, elemental analyses, ^{1}H n.m.r. measurements, optical microscopy, DSC-measurements and X-ray measurements with synchrotron radiation at variable temperatures. If more than 20% of the 4,4′-dihydroxybiphenyl were replaced by isosorbide the copolyesters lost their thermotropic character. All polyesters with 20% or less isosorbide proved to be semicrystalline thermotropic materials showing three phase transitions: firstly a melting process (T_{m1}), secondly a transition from a sanidic LC-phase to a normal nematic or cholesteric melt (T_{m2}) and finally to the isotropisation (Ti). The copolyester containing 10% isosorbide was capable of forming a Grandjean texture. © 1998 Elsevier Science Ltd. All rights reserved.

(Keywords: cholesteric polymers; polycondensation; layer structures)

INTRODUCTION

The present work is part of a broader study of cholesteric polyesters, particularly of polymers containing isosorbide (1,4;3,6-dianhydro-D-sorbitol) or other ‘sugar diols’ as chiral building block. The background of this study is the potential usefulness of cholesteric materials as organic pigments, coloured films, membranes or coatings provided that they fulfill the following requirements[1]. Firstly, they should be capable of forming a Grandjean (GJ) texture[2,3] with a selective reflection of circularly polarized visible light. Secondly, they should enable a fixation of this GJ texture originally formed in the melt, in order to keep it stable under service conditions.

In previous studies we have synthesized and characterized numerous cholesteric polyesters and polycarbonates containing isosorbide or isomannide and various unsubstituted dicarboxylic acids (e.g. **1**)[4–9]. These polyesters or polycarbonates form a normal cholesteric melt and a cholesteric glass in the solid state. Furthermore, we have recently synthesized chiral sanidic polyesters such as **2**[10], which form a chiral LC-phase along with a sanidic layer structure in the solid state. The present work had the purpose to study polyesters of the structure **3** which represent a kind of crossover step between the structures 1 and **2**.

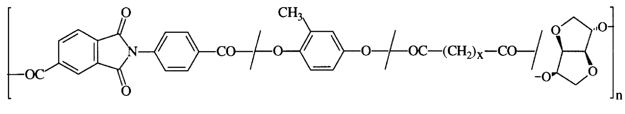

1 (x = 4, 8)

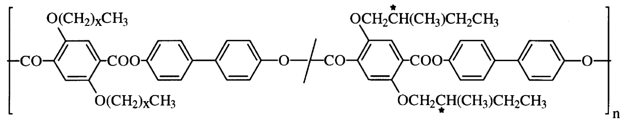

2 (x = 11, 15)

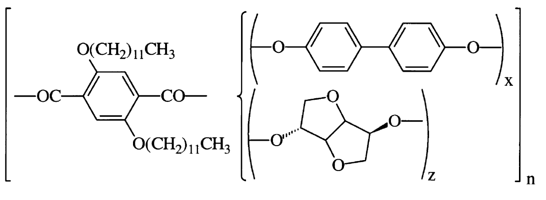

3

a: x/z = ∞/1
b: x/z = 19/1
c: x/z = 9/1
d: x/z = 8/2
e: x/z = 7/3
f: x/z = 5/5

EXPERIMENTAL

Materials

4,4′-dihydroxybiphenyl, diethyl-2,5-dihydroxyterephthalate, dodecylbromide and isosorbide were all purchased from Aldrich Co. (Milwaukee, Wisc. USA) and used as received. 2,5-bis(dodecyloxy)terephthaloylchloride (m.p. 62°C) was prepared according to ref. 11. 4,4′-bistrimethylsiloxybiphenyl was obtained by silylation of DHB with an excess of hexamethyldisilazane in refluxing toluene (m.p. 64°C[12]).

---

* To whom correspondence should be addressed.

Polycondensations

Polycondensation in bulk ('silyl method') (**3a**). 2,5-bis(dodecyloxy)terephthaloylchloride (10 mmol), 4,4′-bistrimethylsiloxybiphenyl (10 mmol) and benzyltriethylammonium chloride (10 mg) were weighed into a cylindrical glass reactor equipped with a mechanical stirrer, gas-inlet and gas-outlet tubes. The reaction vessel was placed into a metal bath preheated to 150°C. The reaction mixture was in the molten state at this temperature and a slow evolution of chlorotrimethylsilane was observed. The temperature was raised in steps of 10°C per 10 min up to a final temperature of 260°C in order to keep the mixture in the molten state. Finally vacuum was applied for 15 min. The cold product was dissolved in a mixture of CH_2Cl_2 and trifluoroacetic acid (TFA) (volume ratio 4:1) and precipitated into cold methanol. The isolated polyester was dried at 80°C for 2 d *in vacuo*.

*Polycondensation in 1-chloronaphthalene (***3a–3f***)*. A cylindrical glass reactor equipped with a mechanical stirrer, gas-inlet and gas-outlet tubes was charged with a solution of the substituted terephthaloylchloride (10 mmol) and 10 mmol of the mixture of the diphenol and isosorbide in 15 ml 1-chloronaphthalene. The reaction vessel was placed into an oil bath preheated to 200°C where the evolution of hydrochloric acid started immediately. The solution was stirred at this temperature for 16 h. After cooling to room temperature the reaction mixture was precipitated into methanol. The isolated polyesters were dried at 80°C for 7 d *in vacuo*. The homopolyester **3a**′ was prepared analogously, but at a reaction temperature of 260°C.

Measurements

The inherent viscosities were measured with an Ubbelohde viscosimeter thermostated at 20°C. The optical rotations were measured with a Perkin Elmer M 241 in cuvette of 10 mm length. The 100 MHz *1*H n.m.r. spectra were recorded with a Bruker AC-100 FT n.m.r. spectrometer in 5 mm o.d. sample tubes. The DSC measurements were conducted with a Perkin Elmer DSC-4 in aluminium pans under nitrogen. The DMA measurements were conducted with a Du Pont DMA 983 in resonance with a sample size of 13.0 × 2.8 mm (l × w × h) and an amplitude of 0.3 mm. The WAXS powder patterns were recorded either with a Siemens D-500 diffractometer using Ni filtered CuKα radiation or by means of synchrotron radiation at HASYLAB, (DESY, Hamburg). A one-dimensional position sensitive detector was used and a heating rate of 10°C/min.

RESULTS AND DISCUSSION

Syntheses

The homopolyester (**3a**) was prepared in two different ways. Firstly, the 2,5-bis(dodecyloxy)terephthaloylchloride was polycondensed with 4,4′-bistrimethylsiloxybiphenyl in bulk (method A). This method has proved its usefulness for successfull syntheses of numerous LC-polyester[7,13,14]. In order to avoid temperatures above 300°C, chloride ions are required as catalyst. A high yield but only a moderate inherent viscosity was obtained for the resulting polyester labeled **3a**′ (*Table 1*). A second synthesis was conducted in such a way that the substituted terephthaloylchloride and free 4,4′-dihydroxybiphenyl were polycondensed in 1-chloronaphthalene at 260°C. This liquid is an inert reaction medium and a good solvent for any kind of polyesters. The resulting polyester **3a** had indeed a considerably higher viscosity value. The influence of the different molecular weights on the phase transitions is discussed below.

The copolyesters were prepared by polycondensations of 2,5-bis(dodecyloxy)terephthaloylchloride with mixtures of isosorbide and free 4,4′-dihydroxybiphenyl in 1-chloronaphthalene. This approach was preferred because silylated isosorbide and 4,4′-bistrimethylsiloxybiphenyl possess largely differing reactivities. We have expected that the copolycondensation of the free diols is more appropriate to obtain random sequences, in as much as the liberated HCl may catalyze transesterification. Furthermore, this method had yielded the higher viscosity in the case of **3a**. In order to avoid HCl catalyzed side reactions of isosorbide the temperature was lowered to 200°C. The yield (and various properties) of all polyesters were summarized in *Table 1*. The yields were all about 95 ± 2% regardless of the

Table 1 Yields and properties of the polyesters **3a**′ and **3a**–**3f**

Polymer [no.]	Synth. method	Yield [%]	η^a_{inh} [dl/g]	$[\alpha^{20}_D]^b$	Elem. formula (form. weight)	Elem. analyses		
							C	H
3a′	A	95	0.54	0	$C_{44}H_{60}O_6$	Calcd.	77.16	8.83
(*x* = 0.00)					(685.0)	Found	76.87	8.88
3a	B	97	3.45	0	$C_{44}H_{60}O_6$	Calcd.	77.16	8.83
(*x* = 0.00)					(685.0)	Found	78.22	8.89
3b	B	98	1.13	−10	$C_{437}H_{600}O_{61}$	Calcd.	76.85	8.86
(*x* = 0.05)					(6829.6)	Found	76.65	8.71
3c	B	98	0.92	−21	$C_{434}H_{600}O_{62}$	Calcd.	76.55	8.88
(*x* = 0.10)					(6809.6)	Found	76.28	8.84
3d	B	98	0.84	−26	$C_{428}H_{600}O_{64}$	Calcd.	75.94	8.93
(*x* = 0.20)					(6769.5)	Found	75.80	8.81
3e	B	93	0.50	−29	$C_{422}H_{600}O_{66}$	Calcd.	75.32	8.99
(*x* = 0.30)					(6729.4)	Found	75.33	8.83
3f	B	97	0.36	−36	$C_{82}H_{120}O_{14}$	Calcd.	74.06	9.10
(*x* = 0.50)					1329.9	Found	73.83	8.81

[a] Measured at 20°C with *c* = 2 g/l in CH_2Cl_2/TFA (volume ratio 4:1).
[b] Measured at 20°C with *c* = 2 g/l in CH_2Cl_2/TFA (volume ratio 7:1).

syntethic method whereas a broader variation was observed for the inherent viscosities. SEC measurements were not conducted, because all polyesters requested an acidic cosolvent for their complete solubility. ^{1}H n.m.r. spectra (an example is presented in *Figure 1*) and the optical rotations listed in *Table 1* proved that isosorbide was incorporated according to the feed ratio.

The phase transitions of the homopolyesters **3a** and **3a′**

The chain packing and thermal properties of the homopolyesters **3a**/**3a′** have already been reported in previous papers[10,15]. The DSC curves displayed in ref. 15 exhibit two endotherms in the heating trace and the corresponding two exotherms in the cooling trace. The first endotherm was reported to indicate the transition from the solid state to a nematic melt, whereas the second endotherm represents the isotropization. These experimental findings and their interpretation were confirmed in the present study, but a more careful reinvestigation revealed an additional phase transition.

As demonstrated by the DSC measurements displayed in *Figure 2* the first heating curve of **3a′** exhibits a weak endotherm at 89°C. Only a flat barely detectable endotherm at this temperature is observed in the second heating trace, whereas the corresponding exotherm is lacking in the cooling curve. In the case of **3a** a flat broad endotherm appears in the first heating curve above 100°C with a maximum at 144°C. Again the corresponding exotherm is not detectable and the endotherm is not clearly reproducible in the second heating curve. These DSC measurements arouse the suspicion that a melting or softening process occurs in the temperature range. The weak and poorly reproducible endotherms could, of course, not serve as convincing evidence. However, examinations of the relatively low molecular weight sample **3a′** by optical microscopy revealed that the phase between 100 and 200°C is slightly mobile under pressure. No mobility was detectable for the high molecular weight sample **3a**. Therefore, films of both samples were pressed above 200°C and subjected to dynamic mechanical analyses (DMA). As illustrated by *Figure 3* for polyester **3a′** both samples behaved as solids up to a temperature around 90° ± 5°C, but began to flow upon further heating. Thus these DMA curves provided a definite prove for a melting process in the temperature range of 80–100°C. As demonstrated by

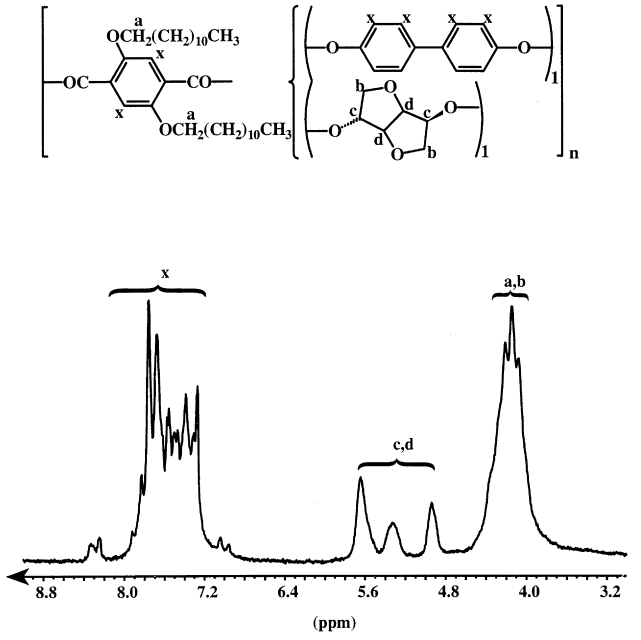

Figure 1 Partial 100 MHz ^{1}H n.m.r. spectrum of the copolyester **3f**

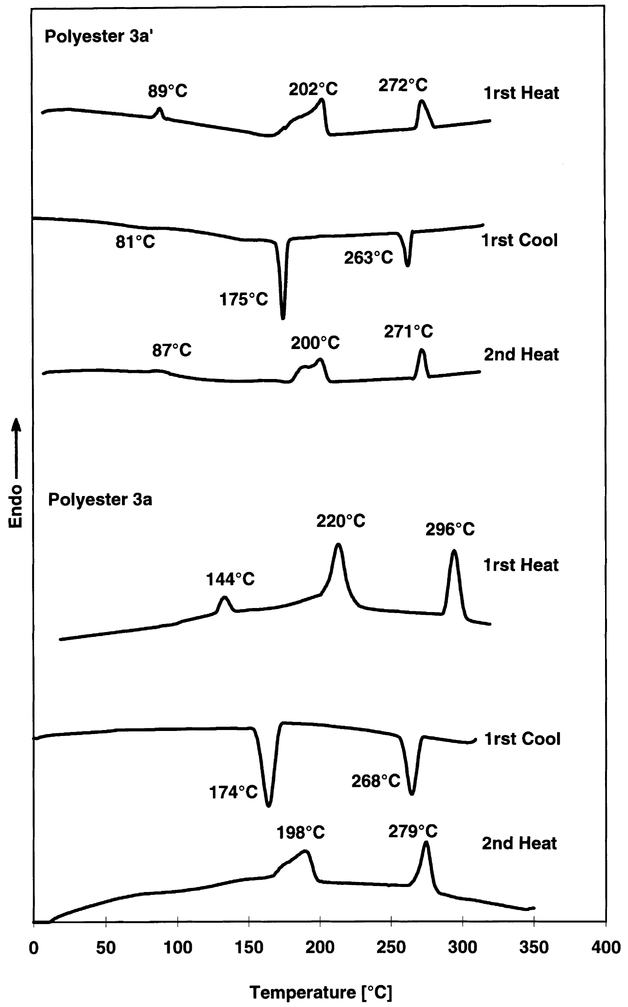

Figure 2 DSC measurements (heating and cooling rate 20°C/min) of the homopolyesters **3a** and **3a′**

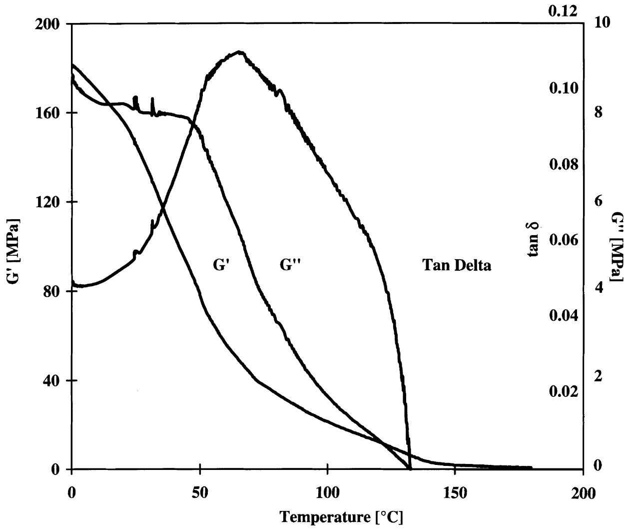

Figure 3 Dynamic mechanical measurement of the homopolyester **3a**

all other endotherms of **3a** and **3a**′ the exact temperature depends on the molecular weight.

For the definition and labeling of the solid phase below 100°C and for the highly viscous phase between 100 and 200°C the WAXS powder patterns recorded at 25°C with CuKα radiation (*Figure 4*) and those recorded with synchrotron radiation up to 220°C, were required. The WAXS powder pattern of **3a**′ is presented in *Figure 4* together with the powder patterns of the copolyesters **3b**, **3c** and **3d**. At room temperature all these WAXS powder patterns show the same structure. A strong middle angle reflection (MAR) is followed by a weak broad second order reflection and a broad intensive 'halo-like' reflection at $2\Theta = 20$–$21°$. The MAR indicates the existence of a sanidic (i.e. board like[16]) layer structure with almost fully extended but interdigitated alkyl side chains according to the scheme of *Figure 5*. The fine structure of the MARs indicating the formation of a 'honey comb' type of layer structure discussed previously[15] was not observed in this work. The synchrotron radiation measurements of **3a**′ conducted with a heating and cooling rate of 10°C/min showed that the MAR vanished at the temperature of the second endotherm (200°C, T_{m2}) and came back upon cooling around 170–180°C (2nd exotherm, see *Figure 2*). The position of the MAR, and thus the *d*-spacing of the layer, did not significantly change, when the temperature was varied. Therefore, the phase between T_{m1} and T_{m2} may be called sanidic liquid-crystalline phase. The texture of this phase depends on the thickness of the layer under investigation, on the temperature and on the mechanical treatment. Yet it is under most circumstances a colourful marble-like or cloudy schlieren texture which is difficult to represent by a black and white picture like that of copolyester **3b** displayed in *Figure 7a*. Above T_{m2} a normal nematic phase is formed which displays a typical threaded schlieren texture as illustrated in a figure in a previous part of this series[10].

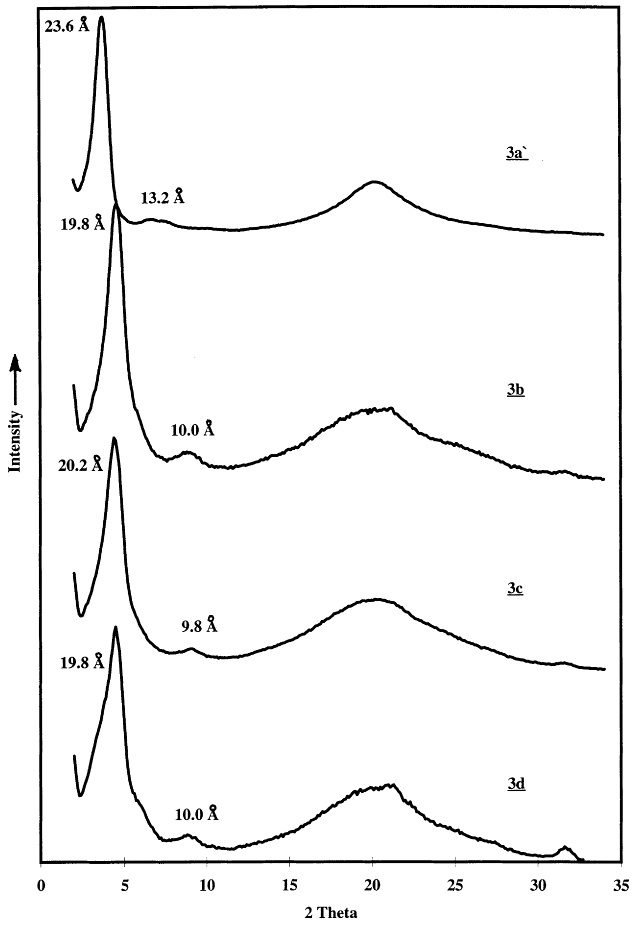

Figure 4 WAXS powder patterns of the copolyesters **3a**′, **3b**, **3c** and **3d**

Finally, the question should be discussed, if a perfect solid sanidic phase shows sharp wide angle reflections. The WAXS powder patterns of **3a**′, **3b**, **3c** and **3d** (*Figure 4*) show that the broad reflection around $2\theta = 20°$ is not a symmetrical 'round curve' as expected for a glassy state even if it is a nematic or smectic glass. The wide angle reflection of **3b**, **3c** or **3d** clearly includes a weak broad additional reflection at $2\theta = 21.5°$ which indicates a low degree of order in the packing of the main chains.

Even if the main chains form rather perfect stacks in terms of the sanidic layer structure, they may internally be disordered in two sort of ways. Firstly, the aromatic rings of one chain will not be all coplanar, but will have different angles of rotation (around their para axes) relative to each other. Secondly, the terephthalate units may adopt a cisoid or transoid conformation (Scheme 1) and both orientations may form a random sequence along the chain. This effect alone suffices to explain the lack of sharp WAXS

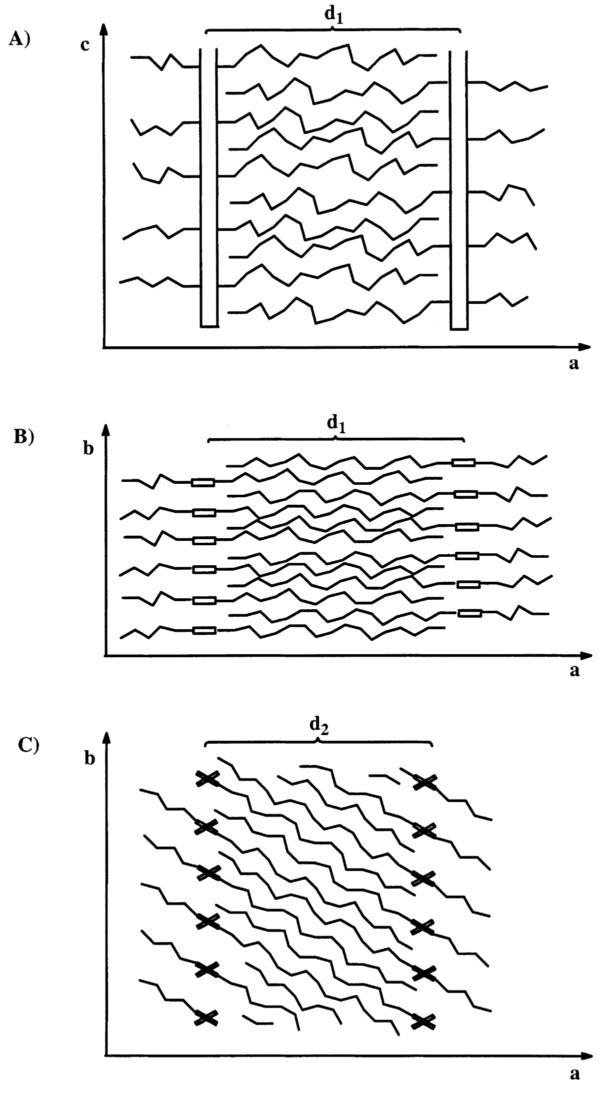

Figure 5 Scheme of a sanidic layer structure with interdigitated alkyl side chains

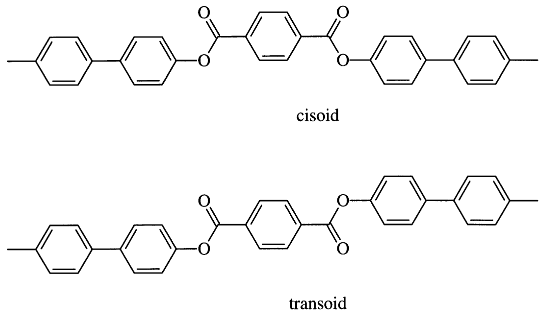

Scheme 1

reflections. We think the best label for this solid state is ‘solid sanidic mesophase’. When compared to the intensively characterized polyester of 2,5-bis(dodecyloxy)-terephthalic acid and hydroquinone[11,17–22] the main difference concerns the ordering of the dodecyl side chains. Due to the length of the biphenyl unit the alkyl chains of **3a**/**3a**′ have more space so that they do not crystallize in contrast to the more densely packed polyesters of hydroquinone.

The phase transitions of the copolyesters **3b**–**3f**

The characterization of the copolyesters **3b**–**3f** revealed that the incorporation of isosorbide dramatically reduces the stability of the sanidic layer structure and of the entire liquid-crystalline properties. When more than 20% of the 4,4′-dihydroxybiphenyl was replaced by isosorbide (i.e. in the case of **3e** and **3f**) both the sanidic layer of the solid state and the liquid crystallinity were lost. In other words, the copolyesters **3e** and **3f** showed the properties of normal isotropic and amorphous polyesters. The only phase transition detectable in the DSC traces was the glass transition (T_g) in the temperature range of 18–27°C (*Table 2*). The WAXS powder patterns of all other copolyesters revealed the existence of a sanidic layer structure in the solid state (*Figure 4*). However in the case of **3d** (20 mol% of isosorbide) only one phase transition (T_{m1}) was detectable in the DSC curves, and the optical microscopy with crossed polarizers indicated that the mobile cholesteric melt formed above T_{m1} vanished at relatively low temperatures (150–170°C). The thermal properties of **3b** and **3c** agreed largely with each other and with those of **3a**/**3a**′ (*Table 2*). The melting process at T_{m1} was barely observable in the DSC curve but it was clearly detected by DMA measurements. The transition from the sanidic LC-phase to the cholesteric melt (T_{m2}), and the isotropisation process shifted to lower temperatures with increasing molar fraction of isosorbide. Despite the similarity of the phase transitions and the liquid-crystalline phases themselves, the details of the sanidic layer structures are different for **3a**/**3a**′ on the one hand and **3b**–**3d** on the other hand. As demonstrated by the WAXS powder patterns of the sanidic phase (*Figure 4*) the layer distance of the copolyester is 3.5–4.0 Å shorter than that of the homopolyesters **3a**/**3a**′. However, no trend is detectable in the series **3a**–**3d**.

Why small amounts of isosorbide (e.g. 5% for **3b**) are capable of inducing such a change is difficult to answer. Two different layer structures characterized by different *d*-spacings have also been found for the homopolyester **2**, $x = 15$, as will be reported in the succeeding part of this series. Furthermore, two *d*-spacings were found in the case of polyesters derived from hydroquinone (**4**)[21]. They were explained by the formation of two layer structures corresponding to the schemes in *Figure 5b,c*. In the case of the polyesters **3a**–**3f** the length of the biphenyl units offers more free space between the stacks of the main chain. Computer modelling of two neighboring stacks demonstrates that now the alkyl chains have enough space for coiling and back folding (including hair pin conformations). ^{13}C n.m.r. CP/MAS spectra or **3a** and **3c** revealed a significant predominance of *gauche–trans* over *trans–trans* conformation in agreement with a coiling of the side chains. The same result was obtained for the polyesters **4** in the tilted array (*Figure 5c*)[21]. Therefore, no decision can be made at this time, whether a layer struture with tilted array of side chains (*Figure 5c*) or with a perpendicular array (*Figure 5b*) and folded or coiled side chains is responsible for the shorter *d*-spacings.

The synchroton radiation measurements at elevated temperatures revealed that the chain packing of **3b**–**3d** is even more complex. The MAR at 20 ± 0.4 Å disappeared at T_{m1} and another MAR appeared up to T_{m2} corresponding to *d*-spacing of 26.0 Å (*Figure 6*). This larger layer structure having presumably fully extended side chains appeared

Table 2 Phase transitions of the polyesters **3a**′ and **3a**–**3f**

Polymer [no.]	Heating cycle	Tg^a [°C]	$T_{m1}{}^a$ [°C]	$T_{m2}{}^a$ [°C]	$T_i{}^a$ [°C]	$T_i{}^b$ [°C]
3a′	1. heat	–	89	202	271	275–285
($x = 0.00$)	2. cool	–	87	200	270	
3a	1. heat	–	(144)	220	296	285–300
($x = 0.00$)	2. cool	–	–	198	279	
3b	1. heat	–	90	189	245	245–258
($x = 0.05$)	2. cool	–	86	187	248	
3c	1. heat	22	91	175	222	218–232
($x = 0.10$)	2. cool	22	84	179	220	
3d	1. heat	28	90	–	165	150–170
($x = 0.20$)	2. cool	27	104	–	-	
3e	1. heat	27	–	–	–	–
($x = 0.30$)	2. cool	19	–	–	–	
3f	1. heat	24	–	–	–	-
($x = 0.50$)	2. cool	18	–	–	–	

[a] From DSC measurements with a heating and cooling rate of 20°C/min.
[b] From optical microscopy with crossed polarizers and a heating rate of 10°C/min.

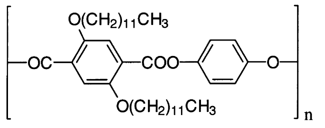

4

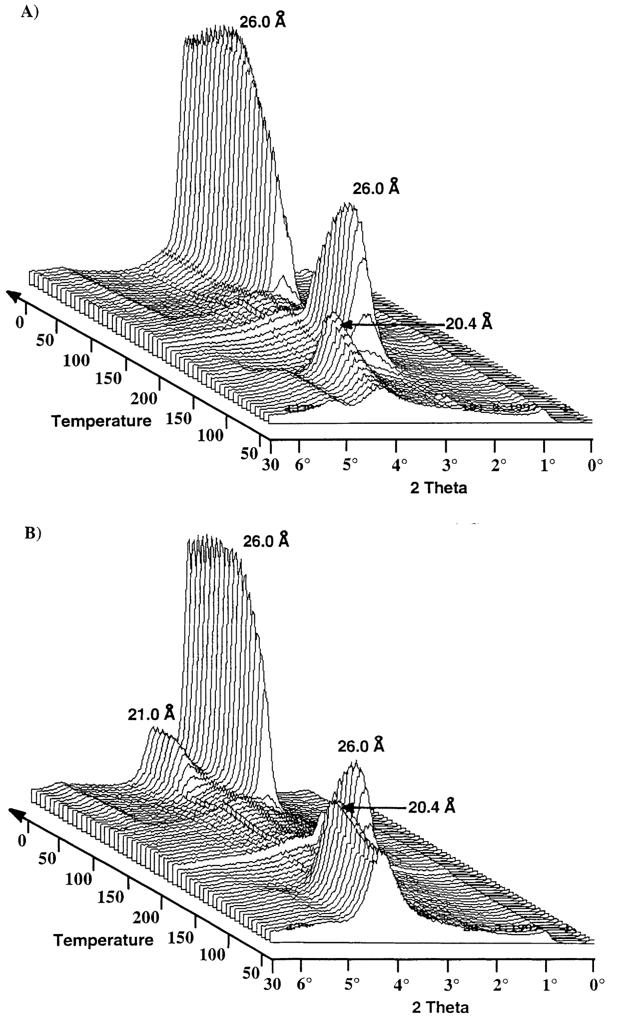

Figure 6 Measurements of the middle angle reflection of (A) copolyester **3b**; and (B) copolyester **3c** with synchroton radiation at a heating and cooling rate of 10°C/min

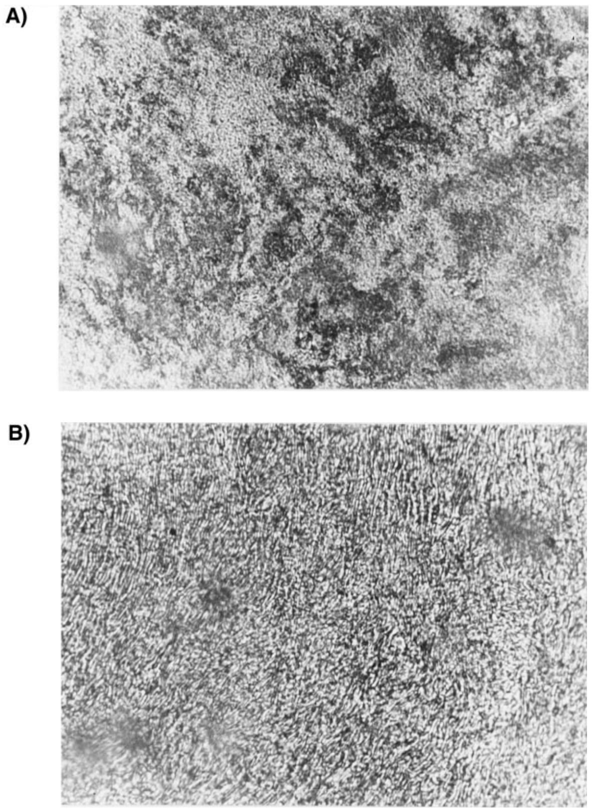

Figure 7 (A) Texture of copolyester (magnification 360) **3b** at 160°C; (B) at 190°C

again upon cooling, and thus seems to be the thermodynamically more stable modification. A similar trend was observed for **3b** and **3c** (*Figure 6*). The modification with a *d*-spacing around 20 ± 0.4 Å changes towards a larger layer structure at T_{m1}. However, upon cooling both layers, the larger one and the more densely packed one, reappeared in the case of **3c**. Both layer distances require an interdigitating of the dodecyl groups, but their conformations are certainly different in both types of layers. The synchroton measurements displayed in *Figure 6* also prove that the chain packing of the copolyesters **3b**–**3d** in the solid mesophase depends on the thermal history.

When examined by optical microscopy with crossed polarizers, a marble like schlieren texture (devoid of black threads) was found for the sanidic LC-phase of **3a**, **3b** and **3c** (*Figure 7A*). Above T_{m2} poorly developed schlieren texture was found. A relatively good example of such a schlieren texture was observed for **3b** immediately above T_{m2} (*Figure 7B*). When the melt of **3b**–**3d** was freely flowing or slightly sheared a rather homogenous texture was obtained. In the case of **3c** intensive shearing yielded a true Grandjean texture, which remained at least partially stable upon rapid cooling (quenching) at room temperature. Such a sheared and quenched film of **3c** was turbid and opalescent due to the sanidic order in the solid state, but it looked greenish on the reflected light and redish in the transmitted light. This result is important, because it proves that the isosorbide interrupts the energetically favorable linear conformation of the main chain to such an extent (possibly favouring hair-pin conformations) that a helical array of chain segments can be formed as it is required of a normal cholesteric phase and for the Grandjean texture. In contrast, the cholesteric sanidic polyesters of structure **2** ($x = 11$) did never yield a Grandjean texture, but they formed an unusual texture (labeled X in ref. 10) which has never been observed in the case of **3b**–**3d**. These results prove that chiral sanidic polyesters of structure **2** ($x = 11$) and **3b**–**3d** possess different optical properties. The absence of a Grandjean texture in the case of the polyesters **2** may be due to an insufficient twisting power of the chiral substituents. However, the existance of texture-X (called 'sausage texture' in future parts of this series) and its absence in the case of the polyesters **3b**–**3d** is difficult to explain without assuming different conformations and spatial arrays for both classes of polyesters. Therefore, the finding that the optical properties of **3b**–**3d** differ largely from those of the polyesters **2** rather supports our previous hypotheses that these rigid rod type polyesters possibly form a chiral nematic phase which is different from a normal cholesteric phase. However, we have to emphasize that our results do certainly not prove this hypotheses yet.

CONCLUSION

The results of the present work clearly indicate (in contrast to the previous study of the copolyester **2**; $x = 12$) that both the homopolyester **3a** and the copolyesters **3b**–**3d**, containing 20 mol% or less of isosorbide, form two liquid-crystalline phases. Upon heating of the solid partially crystalline sanidic mesophase above T_{m1} a highly viscous sanidic liquid-crystalline phase appears. Further heating above T_{m2} yields a normal nematic phase in the case of **3a** or a cholesteric melt in the case of **3b**, **3c** and **3d**. Particularly interesting are the optical properties of these chiral copolyesters, because **3c** is capable of forming a Grandjean texture in contrast to the chiral copolyesters of structure **2**. On the other hand, the so-called 'sausage texture' typical for the chiral copolyester of the structure 2 has never been observed for **3a**–**3c**. These observations suggest that **3a**–**3c** yield a normal cholesteric melt above T_{m2}, because the isosorbide interrupts the stiffness and linear conformation of the main chains. This destabilizing influence has the additional consequence that higher molar fractions of isosorbide ($\geq$ 20 mol%) destroys both the sanidic layer structure in the solid state and the liquid-crystalline character. Obviously, the incorporation of chiral groups into the main chain or into the side chains of poly(4,4′-biphenylene terephthalates) has quite different consequences for the supermolecular structure and for the optical properties.

ACKNOWLEDGEMENTS

We wish to thank the Deutsche Forschungsgemeinschaft for the financial support.

REFERENCES

1. Buning, T. and Kreuzer, F., *Trends Polym. Sci.*, 1995, **3**, 318.
2. Bouligand, Y., *J. Phys.*, 1973, **34**, 603.
3. de Jeu, H. W. and Vertogen, G., in *Thermotropic Liquid Crystalline Fundamentals*. Springer, Berlin, 1977.
4. Kricheldorf, H. R. and Probst, N., *Makromol. Rapid Commun.*, 1995, **16**, 231.
5. Probst, N. and Kricheldorf, H. R., *High Perform. Polym.*, 1995, **7**, 461–471.
6. Kricheldorf, H. R., Berghahn, M., Probst, N., Gurau, M. and Schwarz, G., *Reactive Polym.*, 1996, **30**, 173.
7. Schwarz, G. and Kricheldorf, H. R., *J. Polym. Sci., Part A Polym. Chem.*, 1996, **34**, 603.
8. Kricheldorf, H. R., Sun, S.-J., Gerken, A. and Chang, T.-Ch., *Macromolecules*, 1996, **29**, 8077.
9. Kricheldorf, H.R., Sun, S.-J., Chen, C.-P. and Chang, T.-Ch., *Polym. J. Sci., Part A Polym. Chem.*, 1997, **35**, 1611.
10. Kricheldorf, H.R. and Wulff, D.F., *Polym. J. Sci., Part A Polym. Chem.*, 1997, **35**, 947.
11. Ballauff, M., *Makromol. Chem., Rapid Commun.*, 1986, **7**, 407.
12. Stanley, H., Connel, S. and Winder, J., *J. Org. Chem.*, 1958, **23**, 50.
13. Kricheldorf, H. R., Engelhardt, J. and Weegen-Schulz, B., *Makromol. Chem.*, 1991, **192**, 645.
14. Kricheldorf, H. R. and Domschke, A., *Macromolecules*, 1996, **29**, 1337.
15. Watanabe, J., Sekine, N., Nematsu, T., Sone, M. and Kricheldorf, H. R., *Macromolecules*, 1996, **29**, 4816.
16. Herrmann-Schönherr, O., Wendorff, J., Ringsdorf, H. and Tschirner, P., *Makromol. Chem., Rapid Commun.*, 1986, **8**, 93.
17. Ballauff, M. and Schmidt, G. F., *Makromol. Chem. Rapid Commun.*, 1987, **8**, 93.
18. Ballauff, M. and Schmidt, G. F., *Mol. Cryst. Liq. Cryst.*, 1987, **147**, 163.
19. Berger, K. and Ballauff, M., *Mol. Cryst. Liq. Cryst.*, 1988, **157**, 109.
20. Falk, U. and Spiess, H. W., *Makromol. Chem. Rapid Commun.*, 1989, **10**, 149.
21. Adam, A. and Spiess, H. W., *Makromol. Chem., Rapid Commun.*, 1990, **11**, 249.
22. Schrauwen, C., Pakula, T. and Wegner, G., *Makromol. Chem.*, 1992, **193**, 11.